



All-optical multilevel amplitude regeneration in a single nonlinear optical loop mirror

F. WEN,^{1,2,*} C. P. TSEKREKOS,¹ Y. GENG,² X. ZHOU,² B. WU,² K. QIU,² S. K. TURITSYN,¹ AND S. SYGLETOS¹

¹Aston Institute of Photonic Technologies, Aston University, B4 7ET Birmingham, UK

²Key Lab of Optical Fiber Sensing and Communication Networks, Ministry of Education, University of Electronic Science and Technology of China, 611731 Chengdu, China

*f.wen@aston.ac.uk

Abstract: We experimentally demonstrate all-optical amplitude regeneration of 4-level pulse amplitude modulated signals (PAM4) based on a single nonlinear optical loop mirror (NOLM). Four power-plateau regions are achieved using return-to-zero (RZ) pulses of narrow pulse-width, enabling large nonlinear phase shifts within the highly nonlinear fiber (HNLF). We quantify noise suppression characteristics at each amplitude level and obtain an overall EVM improvement of 0.92dB by optimizing input power and distortion strength. A theoretical analysis has been also carried out matching the experimental results and revealing the design characteristics of the regenerator's nonlinear transfer function.

Published by The Optical Society under the terms of the [Creative Commons Attribution 4.0 License](https://creativecommons.org/licenses/by/4.0/). Further distribution of this work must maintain attribution to the author(s) and the published article's title, journal citation, and DOI.

OCIS codes: (060.1155) All-optical networks; (070.4340) Nonlinear optical signal processing; (190.3270) Kerr effect.

References and links

1. M. A. Sorokina and S. K. Turitsyn, "Regeneration limit of classical Shannon capacity," *Nat. Commun.* **5**, 3861 (2014).
2. J. Kakande, R. Slavík, F. Parmigiani, A. Bogris, D. Syvridis, L. Grüner-Nielsen, R. Phelan, P. Petropoulos, and D. J. Richardson, "Multilevel quantization of optical phase in a novel coherent parametric mixer architecture," *Nat. Photonics* **5**(12), 748–752 (2011).
3. K. Cvecek, K. Sponsel, R. Ludwig, C. Schubert, C. Stephan, G. Onishchukov, B. Schmauss, and G. Leuchs, "2R-regeneration of an 80-Gb/s RZ-DQPSK signal by a nonlinear amplifying loop mirror," *IEEE Photonics Technol. Lett.* **19**(19), 1475–1477 (2007).
4. A. Perentos, S. Fabbri, M. Sorokina, I. D. Phillips, S. K. Turitsyn, A. D. Ellis, and S. Sygletos, "QPSK 3R regenerator using a phase sensitive amplifier," *Opt. Express* **24**(15), 16649–16658 (2016).
5. T. Roethlingshoefer, T. Richter, C. Schubert, G. Onishchukov, B. Schmauss, and G. Leuchs, "All-optical phase-preserving multilevel amplitude regeneration," *Opt. Express* **22**(22), 27077–27085 (2014).
6. M. Sorokina, "Design of multilevel amplitude regenerative system," *Opt. Lett.* **39**(8), 2499–2502 (2014).
7. T. Roethlingshoefer, G. Onishchukov, B. Schmauss, and G. Leuchs, "Cascaded phase-preserving multilevel amplitude regeneration," *Opt. Express* **22**(26), 31729–31734 (2014).
8. F. Wen, S. Sygletos, C. P. Tsekrekos, X. Zhou, Y. Geng, B. Wu, K. Qiu, and S. K. Turitsyn, "Multilevel power transfer function characterization of nonlinear optical loop mirror," in 19th International Conference on Transparent Optical Networks, We.D5.3 (2017).
9. L. Grüner-Nielsen, S. Herstrøm, S. Dasgupta, D. Richardson, D. Jakobsen, C. Lundström, P. A. Andrekson, M. E. V. Pedersen, and B. Pálsdóttir, "Silica-based highly nonlinear fibers with a high SBS threshold," in 2011 IEEE Photonics Society Winter Topical Meeting, TuF2.4 (2015).
10. J. Hansryd, F. Dross, M. Westlund, P. A. Andrekson, and S. N. Knudsen, "Increase of the SBS threshold in a short highly nonlinear fiber by applying a temperature distribution," *J. Lightwave Technol.* **19**(11), 1691–1697 (2001).
11. S. J. Fabbri, S. Sygletos, A. Perentos, E. Pincemin, K. Sugden, and A. D. Ellis, "Experimental implementation of an all-optical interferometric drop, add, and extract multiplexer for superchannels," *J. Lightwave Technol.* **33**(7), 1351–1357 (2015).
12. K. Croussore, C. Kim, and G. Li, "All-Optical regeneration of differential phase-shift keyed signals based on phase-sensitive amplification," *Proc. SPIE* **5814**, 166–175 (2005).
13. Tektronix, "PAM4 signaling in high speed serial technology: test, analysis, and debug," Application Note.
14. M. N. Islam, E. R. Sunderman, R. H. Stolen, W. Pleibel, and J. R. Simpson, "Soliton switching in a fiber nonlinear loop mirror," *Opt. Lett.* **14**(15), 811–813 (1989).

15. F. Wen, M. Sorokina, C. P. Tsekrekos, Y. Geng, X. Zhou, B. Wu, K. Qiu, S. K. Turitsyn, and S. Sygletos, "Phase-preserving multilevel amplitude regeneration in conjugate nonlinear-optical loop mirror pair," in Conference on Lasers and Electro-Optics, SM4K.6 (2018).

1. Introduction

All-optical signal regeneration is a key technology for improving the transmission capacity of future fiber communication systems [1]. Ideally, any proposed regenerator solution should be able to address multilevel signal formats and remove distortion both in amplitude and phase. Removal of the phase distortion has been achieved with phase sensitive amplifiers (PSAs) enabling regenerative operation on up to 4 discrete phase levels [2–4]. On the other hand, nonlinear optical loop mirrors (NOLMs) have been the main approach for amplitude noise suppression, but state of the art experiments have not demonstrated operation for more than 2 amplitude levels [5]. Combining both technologies (PSA and NOLM) in a single subsystem is a promising direction for dealing with complex constellation formats and achieving simultaneous suppression of amplitude and phase distortion [6,7]. In any case, the number of regenerative levels is a critical parameter for the final capacity improvement. For the NOLM scheme in particular, additional efforts are required to overcome current obstacles and improve their multilevel operation.

To increase the number of amplitude regenerative levels in a NOLM, a highly asymmetric configuration of the interferometer is required in combination with high launched signal powers to enable large nonlinear phase difference between the counter-propagating signal components. Unfortunately, stimulated Brillouin scattering (SBS) effects within the highly nonlinear fiber (HNLF) impede the development of the Kerr-based nonlinear response [8]. Although several methods to increase the SBS threshold of the nonlinear medium have been proposed, e.g. applying strain or temperature distribution along the fiber [9,10], these have not been proved adequate to support the requirements of a multilevel operation. On the other hand, due to the low frequency gain of the SBS effect, its influence can be bypassed with the use of return-to-zero (RZ) pulses of narrow pulse-width. Such operation may allow the NOLM to reveal its power oscillatory response, and through further optimization, to fit the purpose of a multilevel regenerator. Compatibility with current non-return-to-zero (NRZ) based highly spectral efficient transmission systems can be maintained through additional NRZ-to-RZ and RZ-to-NRZ photonic conversion circuits [4,11].

In this paper, we perform a thorough theoretical and experimental optimization of the NOLM subsystem to operate as a multilevel amplitude regenerator. Using RZ signals of narrow pulse-width we experimentally obtained a power transfer function (PTF) of four plateau-regions and demonstrated all-optical regeneration of 4-level pulse amplitude modulated signals (PAM4). To the best of our knowledge this is the largest number of regeneration levels achieved with a NOLM. The paper is organized as follows: in section 2, we introduce a simplified subsystem model for the NOLM and perform theoretical optimization of its multiple plateau response. Experimental characterization of the NOLM's PTF curve and investigation of its noise suppression characteristics at each amplitude level are performed in section 3, where we also demonstrate the RZ-PAM4 regeneration. Finally, in section 4 we draw the conclusions of the paper.

2. Operational principle

We developed an analytical model to identify critical design rules for the multilevel operation of the NOLM interferometer. The model was based on the setup of Fig. 1(a). The NOLM comprised an asymmetric optical coupler (OC), a power tuning (PT) device and a HNLF. The first two devices introduced the power asymmetry between the co- and counter-propagating signals, which translated into phase difference by the Kerr effect in the HNLF. In an experimental setup, the OC would be responsible for introducing the coarse asymmetry, whereas the power tuning device (e.g. a variable optical attenuator (VOA) [5,8] or a

bidirectional erbium-doped fiber amplifier (Bi-EDFA) [7]) would enable a finer signal power control. We also had two output signals: one is the transmission signal from the out-port of the OC, and the other is the reflection signal collected at the P3 port of the optical circulator (CIR). Using this simple subsystem model, detailed optimizations on the regenerative performance can be performed. Following the methodology of [12], we derived the reflection power P_{out}^{Ref} and transmission power P_{out}^{Tra} of the NOLM as a function of the input signal power P_{in} :

$$\begin{cases} P_{out}^{Ref} = 2C_p\beta(1-\beta)(1+\cos\Phi_\beta)P_{in} \\ P_{out}^{Tra} = C_p[1-2\beta(1-\beta)(1+\cos\Phi_\beta)]P_{in} \end{cases} \quad (1a),(1b)$$

where $C_p = \exp(2s\delta - \alpha L)$ represents the power tuning parameter, with $s = +/-1$ corresponding to amplification or attenuation, δ is the PT coefficient, α and L are the loss and length of the HNLF. The nonlinear phase is given by $\Phi_\beta = \gamma L[\exp(2s\delta)(1-\beta) - \beta]P_{in}$ where β is the splitting ratio of the OC, and γ is the nonlinear coefficient of the HNLF.

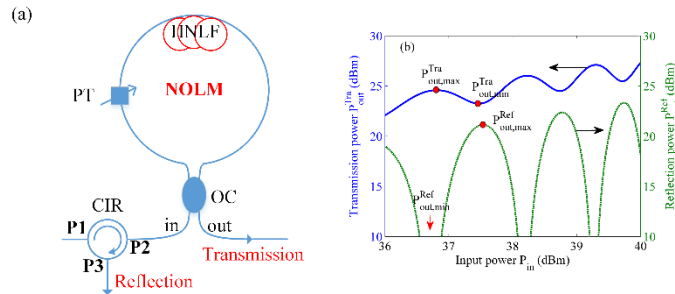


Fig. 1. (a) Setup of a NOLM subsystem, (b) typical PTF curves.

The asymmetry of the configuration leads to different PTFs for the signal at the transmission and the reflection ports, see Fig. 1(b). They are obtained using Eqs. (1)(a) and (b) and reveal the well-known oscillatory behavior of the NOLM interferometer characterized by local minimum and maximum points. Noise suppression is achieved when the amplitude level of the input signal falls within the plateau region of the local maximum point $P_{in,max}^i$ (with $i = Ref$ or Tra), for which a power level of $P_{out,max}^i$ is obtained at the output. Obviously, either the transmission or the reflection port of the NOLM can enable multilevel suppression of noise. However, which port can provide the best and most robust regeneration performance requires further investigation. To this end, we can identify the approximate locations of the local minimum or maximum points $\{P_{in,min}^i, P_{in,max}^i\}$ on the transfer function by solving $1 + \cos\Phi_\beta = \{0, 2\}$, for the reflection port, or the $1 + \cos\Phi_\beta = \{2, 0\}$, for the transmission port, respectively. In all cases, analytical expressions for the input powers are derived, which by replacing in Eqs. (1a) and (1b) we can calculate the corresponding output signal powers $\{P_{out,min}^i, P_{out,max}^i\}$. All the solution sets for the two ports are summarized in Table 1.

Table 1. Local maximum and minimum points

Port	Input	Output
Ref	$P_{in,max}^{Ref} = \frac{2m\pi}{\gamma L [\exp(2s\delta)(1-\beta) - \beta]}$	$P_{out,max}^{Ref} = \frac{8m\pi C_p \beta (1-\beta)}{\gamma L [\exp(2s\delta)(1-\beta) - \beta]}$
	$P_{in,min}^{Ref} = \frac{(2m+1)\pi}{\gamma L [\exp(2s\delta)(1-\beta) - \beta]}$	$P_{out,min}^{Ref} = 0$
Tra	$P_{in,max}^{Tra} = \frac{(2m+1)\pi}{\gamma L [\exp(2s\delta)(1-\beta) - \beta]}$	$P_{out,max}^{Tra} = \frac{C_p (2m+1)\pi}{\gamma L [\exp(2s\delta)(1-\beta) - \beta]}$
	$P_{in,min}^{Tra} = \frac{2m\pi}{\gamma L [\exp(2s\delta)(1-\beta) - \beta]}$	$P_{out,min}^{Tra} = \frac{2m\pi C_p [1-4\beta(1-\beta)]}{\gamma L [\exp(2s\delta)(1-\beta) - \beta]}$

The locations of the power plateaus depend on the interferometer parameters β and δ . The same parameters also affect the width of the plateau regions, which defines the noise suppression capabilities of the regenerator. These dependencies have been investigated in the graphs of Fig. 2, where we have plotted the slope of the PTFs, as a function of the input signal power P_{in} and the splitting ratio β . The slope values have been calculated directly from the logarithmic PTF curve and represent the amplitude noise transfer through the regenerator. The blue colored regions correspond to absolute slope values of less than one, where the amplitude noise suppression takes place. For the reflection port, see Fig. 2(a), we notice a wide operational range for the first plateau region, whereas the higher-order plateaus become significantly narrower due to the strong oscillatory behavior of the PTF. For the transmission port, depicted in Fig. 2(b), wider and of same size plateau widths were calculated when the splitting ratio was higher than 0.9, offering equal noise handling capability to each regenerative level. Consequently, in the experimental design of the regenerator, which is discussed in the following section, we focused on the transmission response and the splitting ratio β of the OC was selected to be 0.9. Furthermore, we investigate the reshaping that is introduced on the PAM4 signal waveform by the nonlinear transfer function of the regenerator at the output of the transmission port. For this, the “level separation mismatch ratio” parameter R_{LM} is used to monitor corresponding nonlinear transformation, defined as [13]: $R_{LM} = 6 \cdot S_{min} / (V_4 - V_1)$, where $S_{min} = 0.5 \cdot \min(V_4 - V_3, V_3 - V_2, V_2 - V_1)$ is half of the swing between the closest adjacent symbols and $V_i (i = 1 \sim 4)$ is the voltage of each amplitude level (see the insert of Fig. 2(c)). The R_{LM} should be one for linear signals. We have plotted the R_{LM} results of transmission signals as a function of the 1st amplitude level V_1 and the level spacing ΔV , see Fig. 2(c), for a splitting ratio β equal to 0.9. The red colored region corresponds to the area where all of input amplitude levels fall into the blue colored regions defined in Fig. 2(b). A maximum R_{LM} value of 0.98 was achieved at $V_1 = 1.28V$ and $\Delta V = 0.46V$, also see the corresponding power levels $P_i (i = 1 \sim 4)$ in the Fig. 2(b). Only a slight reshaping of the original PAM4 waveform was observed. Furthermore, we can identify stationary points on the nonlinear transfer function of the regenerator that enable simultaneous noise suppression and linear conversion of the signal’s amplitude level. However, this requires a slight reshaping of the input PAM4 waveform so that its alphabet points coincide with the stationary points of the regenerator [8].

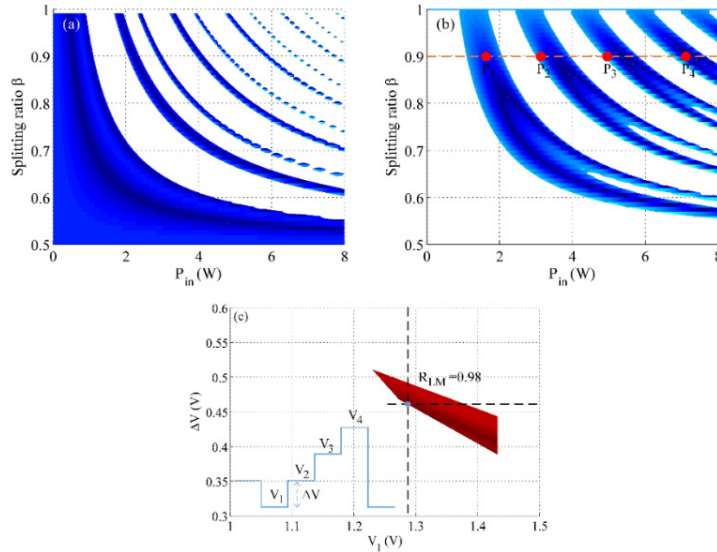


Fig. 2. (a) Reflection and (b) transmission PTF absolute slope values of less than one, (c) R_{LM} results of transmission signal.

3. Experimental setup and results

The all-optical multilevel amplitude regeneration experiment was carried out with the optimized configuration shown in Fig. 3. To bypass the SBS effect, RZ formatted pulses of narrow pulse-width were used. At the transmitter RZ-PAM4 signal generation was achieved as follows: a pulse pattern generator (PPG), triggered by a 10GHz radio frequency (RF) synthesizer, generated a pseudorandom binary sequence (PRBS) NRZ signal with the length of $2^{31}-1$ and an electronic clock. The PRBS-NRZ signal was then fed into a power divider (PD) that had a short connected port C2. Combining the split signal from C1 and the reflected signal from C2 an NRZ-PAM4 electrical signal was obtained at the output port C3, which was used to drive an optical Mach-Zehnder modulator (MZM). The eye diagrams of input electronic NRZ and generated NRZ-PAM4 signals are depicted in Fig. 4. A linear PAM4 signal with the equal level spacing is obtained by using a single PD. The input of the MZM was an optical clock signal of 10ps pulses emitted by a fiber mode-locked laser (MLL) at 1550nm. A tunable optical delay line (TODL) enabled the time alignment of the incoming optical clock pulses with the electrical driving signal. At the output of the transmitter, the generated optical RZ-PAM4 signal was split by a 3dB optical splitter (OS): one part was used for monitoring and the other part was launched into the NOLM regenerator. At the regenerator, the signal power was firstly amplified by a high-power EDFA (HP-EDFA) with a saturation power of 36.5dBm, while the use of an optical isolator (ISO) prevented unwanted back-propagation of the light to the transmitter. The NOLM subsystem comprised a 90:10 OC, a polarization controller (PC), a VOA, a 606m-length strained aluminous-silicate HNLF and a 99:1 OS. The nonlinear coefficient of the HNLF was $7W^{-1}/km$ and the total fiber loss was 12dB. The high loss factor of the fiber used required high operating power levels. One can expect a more power efficient demonstration with the use of a less loss fiber technology, e.g. Ge-doped HNLF. The exact launched power into HNLF was measured by a power meter (PM) at the 1% output port of the OS. The PC was used to optimize the initial state of the interferometer. At the transmission port, the regenerated signal was detected by a 32GHz optical photodiode, and the signal quality was calculated using the sampling data from the oscilloscope.

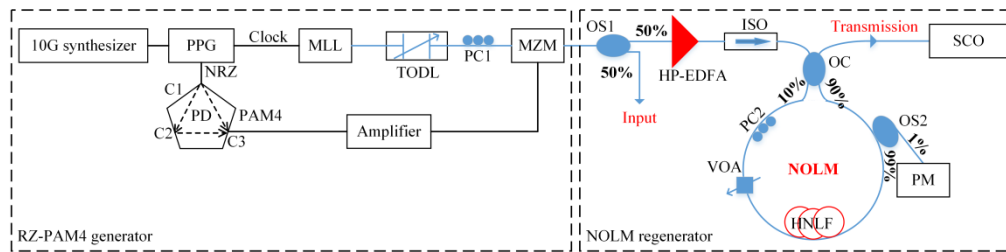


Fig. 3. Experimental setup of all-optical RZ-PAM4 regeneration in a single NOLM subsystem.

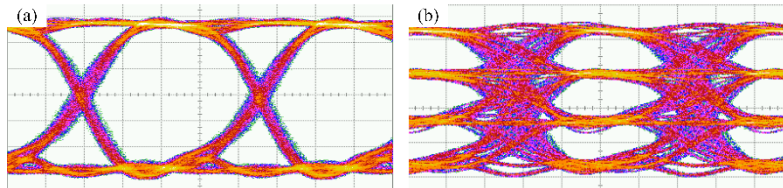


Fig. 4. Eye diagrams of (a) electronic NRZ and (b) NRZ-PAM4 signals.

To identify the optimum operating conditions of the NOLM for multilevel operation, we went through a detailed experimental characterization of its nonlinear response. Initially, we measured the PTF and from there we extrapolated the normalized slope curve. This allowed us to identify the locations of the regenerative regions and to evaluate their corresponding width. To achieve this we launched an un-modulated optical signal (clock) directly into the NOLM and by sweeping the average power of the HP-EDFA we measured the corresponding average power at the output of the transmission port. The resulted PTF and the slope curves are depicted in Fig. 5(a). Four power plateau regions were obtained defined by slope values of less than one. The plateaus were located at 22.5, 25.77, 27.61 and 28.9dBm of input powers, respectively. The extrapolated slope values reflect the noise suppression capability of the regenerator with smaller slope values enabling a more efficient suppression of the distortion. In the same figure we also plotted the theoretically calculated curves, using Eq. (1)(b). Very good agreement between theory and experiment was observed in the first two plateaus. The divergence happened in higher-order plateaus comes from the incomplete-switching-induced pulse distortion for high pump powers [14]. We also notice that the 1st and the 2nd plateau regions were discrete and fully isolated one from the other by high slope values. On the other hand, the boundary between the 3rd and the 4th plateau regions was less clear.

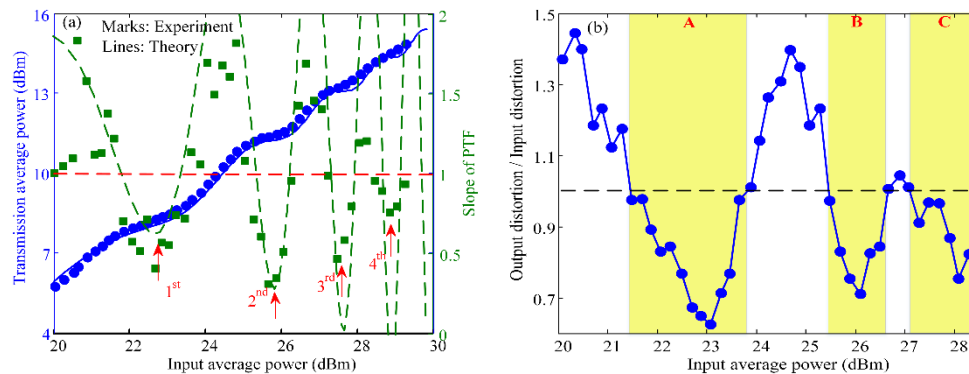


Fig. 5. (a) PTF and its slope of the transmission response. The red arrows indicate four power plateau regions. (b) Corresponding amplitude noise transfer vs. input powers.

The PTF was derived by measuring the average signal power. However, one might expect that this is inadequate for characterizing the multilevel regenerative properties of the NOLM

as its strong nonlinear response might alter severely the shape of output signal pulses. Therefore, we performed an additional characterization of the regeneration performance by measuring the level of the achieved amplitude noise suppression. Specifically, we launched into the regenerator an optical clock distorted by an electrical PRBS ($2^{31}-1$) signal and we characterized the noise suppression as a function of the launched average optical power. Figure 5(b) depicts the peak-to-peak variation of the distortion normalized to the mean peak amplitude values of the clock pulses. In all measurements the received signal power was kept fixed at -10dBm . We notice that the enhancement or suppression of the distortion followed, to a good extent, the PTF slope of Fig. 5(a). However, that fact that the input optical signal is now carrying an amplitude distortion creates a slight shift in the location of the local minimum. Furthermore, the first two suppression regions were clearly observed due to their broader width, whereas the 3rd and the 4th plateau regions appeared combined. Therefore, three regenerative regions, A, B and C with local minimum located at 23.07, 26.01, 28.08dBm, were considered in the proposed NOLM-based regenerator, see Fig. 5(b).

The next step was to investigate more thoroughly the achieved suppression in each one of the three regenerative regions for different amounts of introduced amplitude distortion. Figure 6 depicts the normalized amplitude distortion at the output of the regenerator as a function of the normalized input distortion. The points below the diagonal line designate that amplitude suppression has been achieved. Each regenerative region exhibits a different noise handling capability. We notice that for a normalized amplitude distortion range between 0.276 and 0.62 we could have noise suppression simultaneously on the three regions. The upper limit was set by region B, whereas the lower limit was set by region C. Finally, it is obvious that region A has a much wider capability of suppressing amplitude noise.

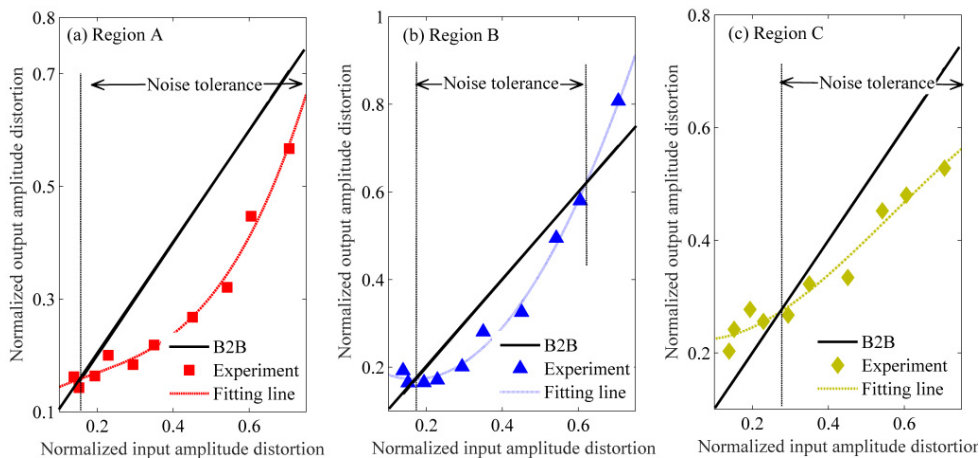


Fig. 6. Noise suppression capability for (a) region A, (b) region B and (c) region C.

Then, all-optical multilevel amplitude regeneration on a RZ-PAM4 signal was demonstrated in this NOLM subsystem. We tuned the TODL to introduce the amplitude distortion by sampling different part of the electronic NRZ-PAM4 signal, and then put the noisy RZ-PAM4 signal into the multilevel regenerator. By adjusting the average power level at the input of the NOLM an optimum operating point could be identified at 24.08dBm, which could provide an overall EVM improvement of 0.88dB, see Fig. 7(a). The EVM is calculated according to the mean values of the received symbols in the four constellation points. At the optimum input power point we characterized the regenerative performance as a function of the input signal distortion, see Fig. 7(b). A maximum EVM improvement of 0.92dB was obtained when the quality of the input signal was characterized by -20.5dB . The power histograms of Fig. 7(b) confirm the noise suppression that achieved at these levels. No

regeneration was observed for input EVM lower than -21.5dB due to the residual ASE noise created within the regenerator subsystem by the HP-EDFA. By degrading the input signal quality above -20.5dB the corresponding EVM-improvement at the output becomes smaller due to the limited noise suppression capability of each regenerative amplitude level. We also carried out the numerical investigation and obtained the similar EVM results with input powers and distortion strengths, see blue lines in Figs. 7(a) and 7(b). Typical eye diagrams of distorted and regenerated RZ-PAM4 signals are depicted in Fig. 8, showing that the pulses maintain their shape. We used the R_{LM} to monitor the reshaping before and after the regenerator. Only 0.8% distortion was observed enabling a cascaded operation. Moreover, we have performed Monte Carlo simulations and evaluated the regenerative performance through direct error counting. In those calculations the experimentally verified transfer function of the regenerator was used. We have evaluated the performance of our regenerator as a decision element before the optical receiver. We notice almost the same bit-error rate (BER) performance between the input and output, check black and blue curves in Fig. 7(c), which proves that the regenerator behaves as an ideal decision element, despite its different nonlinear transfer function. Also, placing the regenerator in the middle of the transmission link can introduce a signal-to-noise ratio (SNR) improvement of approximately 1dB, compared to the un-regenerated case. This relative improvement can become higher for larger system cascades.

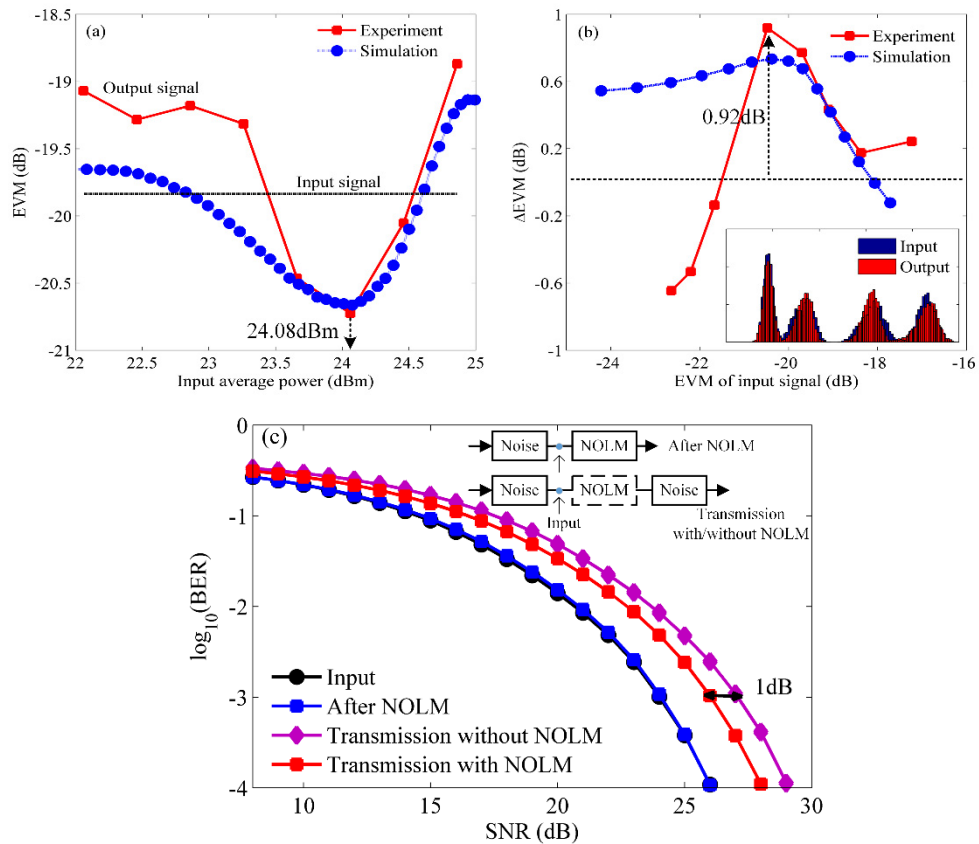


Fig. 7. (a) Input power optimization, (b) EVM improvement for the NOLM regenerator, and power histograms before and after the regeneration, (c) BER simulation results of input and output of the NOLM, transmission with/without the NOLM.

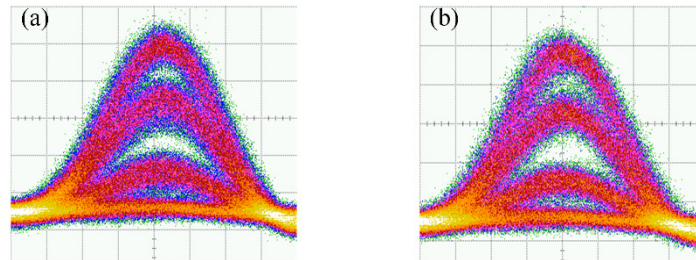


Fig. 8. Eye diagrams of (a) distorted and (b) regenerated RZ-PAM4 signals.

Finally, we note that this NOLM configuration is not phase preserving, but due to self-phase modulation it introduces a different phase shift on each amplitude level of the incoming signal, see parameter Φ_β in Eq. (1). For the case of the PAM4 signal the corresponding phase rotations have been calculated to be 0.038, 0.409, 2.124 and 4.55rad. This might be highly detrimental in a system of cascaded regenerative links. However, we can achieve phase preserving operation in those cases by combining NOLM based regeneration and optical phase conjugation along the link, as it has been initially proposed in [6] and elaborated further in [15].

4. Conclusions

We have designed and demonstrated, to the best of our knowledge, the first experimental implementation of an all-optical amplitude regenerator for RZ-PAM4 signals using a single NOLM setup. Adopting narrow RZ pulses allowed to bypass the influence of the SBS effect in the HNLF and to enable four power-plateau regions in the transfer function. A thorough investigation was also carried out to identify the actual regenerative regions and characterize their noise handling capabilities. Multilevel amplitude regeneration was achieved with an EVM improvement of 0.92dB. Exhibiting more regenerative amplitude levels in the NOLM helps to support transmission links of higher capacity.

Funding

EPSRC project UNLOC (EP/J017582/1); National Natural Science Foundation of China (61505021, 61671108); Marie Skłodowska-Curie Action (701770-INNOVATION); General Project of Sichuan Provincial Education Department (18ZB0235); 111 Project (B14039).

Acknowledgments

The authors would like to thank the Tyndall National Institute for the loan of the highly nonlinear fiber, and A. Ellis, I. Phillips, M. Stephens, M. Sorokina and F. Ferreira for valuable discussions.